

## Catastrophic transition between dynamical patterns in a phonon laser

Qing Lin<sup>1</sup>, Bing He<sup>2,\*</sup> and Min Xiao<sup>3</sup><sup>1</sup>Fujian Key Laboratory of Light Propagation and Transformation, College of Information Science and Engineering, Huaqiao University, Xiamen 361021, China<sup>2</sup>Center for Quantum Optics and Quantum Information, Universidad Mayor, Camino La Pirámide 5750, Huechuraba, Chile<sup>3</sup>Department of Physics, University of Arkansas, Fayetteville, Arkansas 72701, USA

(Received 5 January 2021; accepted 12 July 2021; published 26 July 2021)

The bifurcations or transitions of the classical nonlinear systems with finite degrees of freedom exhibit some dynamical behaviors that are similar to those in the phase transitions of many-body systems. A dynamical type of them in the form of a sudden transition of the amplitudes between two harmonic oscillations, which are stable under periodically driving force, is not so common to see. We show that a sudden transition of this type can be realized in a system of coupling a microresonator that supports a mechanical vibration to another microresonator, and the system was experimentally demonstrated as a phonon laser. If the pump laser power or the intercavity coupling strength is adjusted to a critical value, the cavity field patterns will suddenly change, together with a jump of the stabilized mechanical amplitude. Such transition can be applied to a precise measurement of the optomechanical coupling constant, which is hard to measure due to its proportion to a tiny zero-point mechanical fluctuation amplitude.

DOI: [10.1103/PhysRevResearch.3.L032018](https://doi.org/10.1103/PhysRevResearch.3.L032018)

The phenomena bearing similarity to the phase transitions of many-body systems exist in the few-body systems of nonlinear dynamics [1,2]. A particle moving in a potential with two stable equilibria, for example, undergoes such transition termed bifurcation when the two equilibria degenerate into one due to varying a control parameter. Near the transition point the perturbed particle takes a much longer time to return to equilibrium, a phenomenon known as critical slowing down [3,4], which was observed with optical bistability [5,6] and also exists in chaotic systems [7,8]. Nonlinear dynamical systems can also stabilize on periodic orbits [1,9–20], and the bifurcations involving such limit cycles of dynamical evolutions were previously seen in mode-locked lasers [21,22], nonlinear resonators [23,24], and lasers with feedback [25]. The most complicated bifurcations among them are those of coexisting multiple limit cycles [26–29]. To a planar system, for instance, a transition between two limit cycles is possible only when one of them is unstable. Beyond the mathematical understandings, the direct transitions between deterministic orbits due to changing the system parameters have been rarely encountered in the realistic classical or semiclassical systems with finite degrees of freedom. Except for a few recent examples in the semiclassical context [30,31], the currently ongoing research on nonequilibrium transitions mostly concerns the driven open quantum systems or the hybrid systems with atomic ensemble (see, e.g., [32–38]).

Here we demonstrate that a special kind of transition between two stable limit cycles is realizable in a system illustrated in Fig. 1(a). An optical resonator can be slightly deformed under the radiation pressure [39], to have its wall stabilized in stationary oscillation when the external driving field is blue-detuned [40–46]. By coupling this whispering-gallery-mode microresonator  $\mu R_1$  to another  $\mu R_2$  that may contain optical gain medium, the two coupled cavity field modes can enjoy the parity-time ( $\mathcal{PT}$ ) symmetry and the system thus exhibits plenty of interesting properties [47,48]. The stimulated amplification of the mechanical oscillation on  $\mu R_1$  can be realized under certain conditions, making a type of phonon laser [49–55], which has been experimentally demonstrated [49,56,57]. We here explore a previously unknown phenomenon in the system—a sudden transition of the cavity fields and mechanical oscillation due to varying the system parameters.

The system in Fig. 1(a) has the following elements: (1) the field in  $\mu R_1$  exerts a radiation pressure proportional to the constant  $g_m$  on the mechanical mode, while it linearly couples to the field in  $\mu R_2$  with a coupling rate  $J$ ; (2) relative to  $\mu R_1$  with the damping rate  $\kappa = \kappa_e + \kappa_i$  ( $\kappa_e$  is the coupling rate to the pump laser and  $\kappa_i$  the intrinsic cavity loss), the pump laser with the amplitude  $E = \sqrt{\kappa_e P / (\hbar \omega_l)}$  ( $P$  is the laser power and  $\omega_l$  the laser frequency) has its detuning fixed at the point  $\Delta = \omega_c - \omega_l = -\omega_m$ ; (3) inside  $\mu R_2$  with the total damping rate  $\gamma$ , the optical gain  $g(t)$  saturates from the initial value  $g_0$  and at a speed indicated by the dimensionless rate  $I_S$  [58,59]. Then, in terms of the dimensionless quadratures  $X_{c,1(2)}$  and  $P_{c,1(2)}$  of a cavity field, which contribute to the field intensity  $I_{1(2)} = \frac{1}{2}(X_{c,1(2)}^2 + P_{c,1(2)}^2)$  equivalent to the cavity photon number, together with the dimensionless mechanical displacement  $X_m$  [differed from the real one by the factor  $\sqrt{\hbar/(m\omega_m)}$  determined by the effective mass  $m$  and

\*bing.he@umayor.cl

Published by the American Physical Society under the terms of the Creative Commons Attribution 4.0 International license. Further distribution of this work must maintain attribution to the author(s) and the published article's title, journal citation, and DOI.

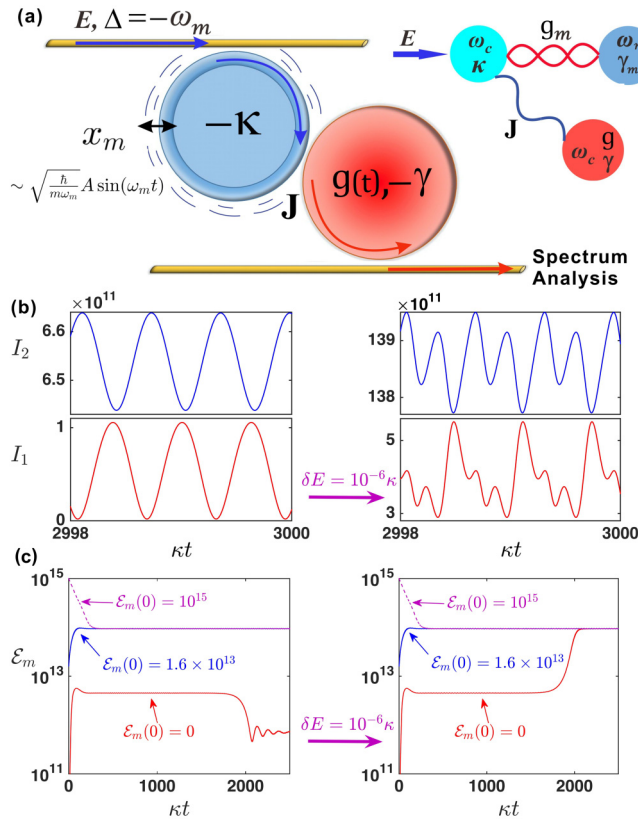


FIG. 1. (a) A system of coupled microresonators similar to some experimental phonon laser setups [49,56,57]. The mechanical motion  $x_m(t)$  on  $\mu R_1$  stabilizes to an oscillation (an exaggerated view is given here). The coupling strength  $J$  is adjustable by the gap distance between  $\mu R_1$  and  $\mu R_2$ . (b) The change of the stable cavity field patterns due to a small increase from  $E = 1837165.781145\kappa$  to  $E = 1837165.781146\kappa$ . The single-frequency pattern before the transition is due to the optical gain, which makes  $I_2$  higher than  $I_1$  on both sides of the transition. The simulations are performed with an initially static mechanical mode of  $\mathcal{E}_m(0) = 0$ .  $\kappa t$  is the dimensionless time scale. (c) The corresponding effect on the evolution paths for the mechanical energy  $\mathcal{E}_m = \frac{1}{2}(X_m^2 + P_m^2)$ , a dimensionless quantity equivalent to a phonon number. The used system parameters:  $g_m = 2 \times 10^{-6}\kappa$ ,  $\omega_m = 10\kappa$ ,  $\gamma = 0.01\kappa$ ,  $g_0 = 2\kappa$ ,  $I_s = 10^{10}$ ,  $\gamma_m = 0.01\kappa$ , and  $J = 0.3\kappa$ .

the mechanical frequency  $\omega_m$ ] and dimensionless mechanical momentum  $P_m$ , one has the following dynamical equations:

$$\begin{aligned} \dot{X}_{c,1} &= -\kappa X_{c,1} - g_m X_m P_{c,1} + J P_{c,2} + \sqrt{2}E \cos(\omega_m t), \\ \dot{P}_{c,1} &= -\kappa P_{c,1} + g_m X_m X_{c,1} - J X_{c,2} - \sqrt{2}E \sin(\omega_m t); \end{aligned} \quad (1)$$

$$\begin{aligned} \dot{X}_m &= \omega_m P_m, \\ \dot{P}_m &= -\omega_m X_m - \gamma_m P_m + \frac{1}{2}g_m(X_{c,1}^2 + P_{c,1}^2); \end{aligned} \quad (2)$$

$$\begin{aligned} \dot{X}_{c,2} &= -\gamma X_{c,2} + \frac{g_0}{1 + \frac{X_{c,2}^2 + P_{c,2}^2}{2I_s}} X_{c,2} + J P_{c,1}, \\ \dot{P}_{c,2} &= -\gamma P_{c,2} + \frac{g_0}{1 + \frac{X_{c,2}^2 + P_{c,2}^2}{2I_s}} P_{c,2} - J X_{c,1}, \end{aligned} \quad (3)$$

given in the reference frame rotating at the resonance frequency  $\omega_c$  of  $\mu R_{1(2)}$ . The numerical simulations with Eqs. (1)–(3) are performed with the system parameters scaled with respect to the damping rate  $\kappa$  of  $\mu R_1$ .

We start from a single microresonator  $\mu R_1$  ( $J = 0$ ). If the pump power goes up across a threshold, its supported mechanical mode will stabilize to an oscillation (the initial phase is chosen to be zero) [45]

$$X_m(t) = A \sin(\omega_m t) + d \quad (4)$$

with the amplitude  $A$  and a small displacement  $d$  under the radiation pressure, instead of slowing down to a standstill. Across this point of supercritical Andronov-Hopf bifurcation for the mechanical mode, the cavity field quadrature will become

$$\begin{aligned} X_c(t) \sim \sum_{n=-\infty}^{\infty} \left\{ \frac{\kappa J_n(-\frac{g_m A}{\omega_m})}{(n\omega_m + \Delta)^2 + \kappa^2} E \cos(n\omega_m t) \right. \\ \left. + \frac{(n\omega_m + \Delta) J_n(-\frac{g_m A}{\omega_m})}{(n\omega_m + \Delta)^2 + \kappa^2} E \sin(n\omega_m t) \right\}, \end{aligned} \quad (5)$$

with its harmonic components ( $n \geq 1$ ) gradually appearing with the continuous increase of the mechanical amplitude  $A$  from zero, where  $J_n(x)$  is the Bessel function of the first kind. Such a gradual change from a static cavity field intensity to an oscillation spectrum of  $n\omega_m$  is like a generalized Neimark-Sacker bifurcation that brings about the extra frequency components. However, this smooth transition will be gone once another microresonator  $\mu R_2$  is coupled to  $\mu R_1$ . Then, as in Fig. 1(b), only a tiny pump power increase  $\delta P \sim \hbar\omega_l\kappa$  (in the order of picowatt if  $\kappa \sim 100$  MHz and  $\omega_l$  is an optical frequency) across a certain point will lead to a multifrequency cavity field, which is much stronger than the single-frequency one induced by the optical gain before the transition. Meanwhile, as shown in Fig. 1(c), the mechanical mode initially with  $\mathcal{E}_m(0) = 0$  will evolve to an orbit with  $\langle \mathcal{E}_m \rangle \approx 9.4 \times 10^{13}$ , higher than the one with  $\langle \mathcal{E}_m \rangle \approx 7.2 \times 10^{11}$  before the transition.

A model of three coupled oscillators, respectively representing the cavity and mechanical modes, abstracts the setup in Fig. 1(a). One of the oscillators ( $\mu R_1$ ) interacts with the mechanical one through the cubic potential  $-\frac{1}{2}g_m X_m(X_{c,1}^2 + P_{c,1}^2)$  and couples to another oscillator ( $\mu R_2$ ) through the quadratic potential  $J(X_{c,1}X_{c,2} + P_{c,1}P_{c,2})$ . The former interaction proportional to the small constant  $g_m$  is enhanced by the pump field with the amplitude  $E$  [39–46,60]. The dominance of the latter in the limit of large  $J$  reduces the system to a linear coupler with negligible optomechanical interaction. The balance of these two competing factors will be tipped if  $E$  or  $J$  goes across a critical value, to give rise to a sudden transition depicted in Figs. 1(b) and 1(c).

Because the dynamical evolutions of the three parts of the coupled system proceed together, one can see the overall picture from a subsystem. The resonance effect of the cavity field component with the frequency  $\omega_m$  leads to a simple form of the stabilized mechanical motion in Eq. (4), so it is convenient to follow the mechanical oscillator for the purpose. To this model of dynamical system, the mechanical oscillator can be hit at  $t = 0$ , to gain the different initial conditions

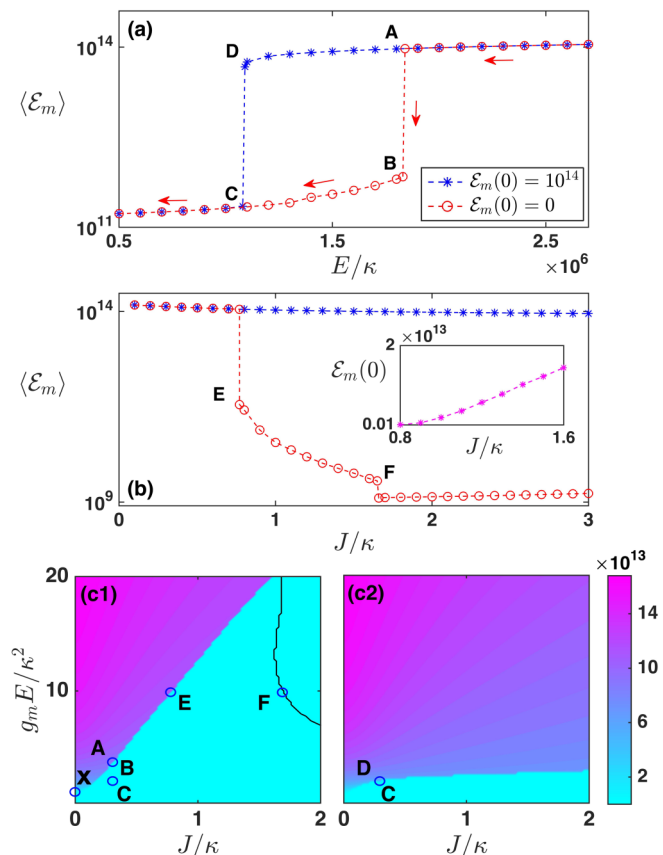


FIG. 2. (a) The evolved time-average mechanical energy under a fixed cavity coupling  $J = 0.3\kappa$ , for two different values of  $\mathcal{E}_m(0)$ . (b) The evolved time-average mechanical energy under the condition  $g_mE = 10\kappa^2$ , for the same values of  $\mathcal{E}_m(0)$  in (a). (c1) The distribution of the evolved time-average mechanical energy from  $\mathcal{E}_m(0) = 0$ . (c2) The changed distribution of the sudden transition boundary due to  $\mathcal{E}_m(0) = 10^{14}$ . The fixed parameters are the same as those in Fig. 1.

as those displayed in Fig. 1(c), which can make the sudden transition occur at different critical values  $E_c$ . One example is in Fig. 2(a): the oscillator with  $\mathcal{E}_m(0) = 10^{14}$  evolves to a higher orbit at point C, where the pump drive amplitude is lower than that at point B, the transition point under the condition  $\mathcal{E}_m(0) = 0$ ; the comparison is seen more clearly from the evolved mechanical energy distributions in Figs. 2(c1) and 2(c2), where point B and point C are on the different boundaries of sudden transition. Point B is a limit point where the oscillator under any initial condition must evolve to the higher orbit, which is detectable by the corresponding cavity field pattern. The arrowed trajectory without lagging behind toward point D indicates that the evolution from a fixed initial condition does not display a hysteresis in the parameter space.

The orbits at any  $J \neq 0$  inherit the stability of the limit cycles from a supercritical Andronov-Hopf bifurcation at  $J = 0$  [the part above point “X” in Fig. 2(c1)]. Such stability can be also seen from the equation

$$\delta\ddot{X}_m + \gamma_m\delta\dot{X}_m + \omega_m^2\delta X_m = g_m\omega_m\delta I_1 \quad (6)$$

governing the behavior of a small deviation from a mechanical orbit.  $\delta X_m$  responding linearly to  $\delta I_1$  will not diverge unless the field intensity in  $\mu R_1$  suddenly jumps to a higher value.

From the left side of Fig. 2(b) there comes a trajectory of the stable orbits from the unique stable limit cycle at  $J = 0$ . It splits into two parts with a sudden transition when  $J$  reaches the value at point “E,” from which all those with the initial energy  $\mathcal{E}_m(0) < 1.6 \times 10^{11}$  will evolve to the lower stable orbit. In the parameter space such splitting of the orbit occurs on the diagonal boundary in Fig. 2(c1). The required initial mechanical energy  $\mathcal{E}_m(0)$  for maintaining on the higher orbit goes up quasilinearly with  $J$ , as shown in the inset of Fig. 2(b), so that the higher one will gradually disappear where the two microresonators are strongly coupled. Across point F in Fig. 2(b), another sudden transition turns the oscillating pattern induced by the optical gain [58,59] into a static pattern for  $\mathcal{E}_m$ , and the boundary on which the point locates is delineated by a black curve in Fig. 2(c1).

Our concerned sudden transition between two stable orbits, both of which are equivalent to the form in Eq. (4), resembles the catastrophic bifurcations between two stable equilibria [4]. However, in addition to the fact that an unstable equilibrium also exists in a catastrophic bifurcation, the location of the transition, as exemplified by the sudden jump boundaries in Figs. 2(c1) and 2(c2), is relevant to the system’s initial condition. To such a nonlinear coupler under external driving, its limit cycles in the phase space are determined by the system parameters, but whether the higher orbit can be reached on the right side of the diagonal boundary in Fig. 2(c1) depends on its initial energy. The existing initial condition should be considered in an experiment of slowly varying the pump power toward the transition point.

A phenomenon of critical slowing down associated with the sudden transition distinguishes it from those due to crossing the exceptional points (somewhere the system’s eigenstates have a qualitative change) [61–64] of the  $\mathcal{PT}$ -symmetric systems of coupled cavities. To capture the essential features, we simply look at the phenomenon without optical gain, like the phonon laser setups reported in Refs. [49] and [57]. The numerical simulations displayed in Figs. 3(a1) and 3(a2) show the different critical behaviors at  $J \neq 0$  from those near the Andronov-Hopf bifurcation at  $J = 0$ . From the same distance  $E - E_c < 0$  before a transition point, the slowing down is intensified by the coupling with  $\mu R_2$ . However, across the transition point to  $E > E_c$ , the tendency is reversed and the finally evolved orbits for the different  $E$  become very close to each other, indicating a distinction of the limit cycle size at  $J = 0$ . Two critical exponents  $\eta$  and  $\delta$  quantify the altered critical dynamics by  $\mu R_2$ , to have the power laws

$$\begin{aligned} t_{st} &\sim (J_c - J)^{-\eta} & (J < J_c), \\ t_d &\sim (J - J_c)^{-\delta} & (J > J_c) \end{aligned} \quad (7)$$

for the evolution timescales toward stability, where  $t_{st}$  is the time for the system to stabilize, and  $t_d$  for the field intensities to decay to  $e^{-1}$  of the maximum indicates the evolution speed on the other side of the transition (the practice is similar to the one in Ref. [8]). The linear relations between  $\log(\kappa t_{st(d)})$  and  $\log|(J - J_c)/J_c|$ , obtained from the numerical calculations with some different  $J_c$  as in Figs. 3(b1) and 3(b2), give the exponents  $\eta = 0.901$  and  $\delta = 0.964$  as the slopes.

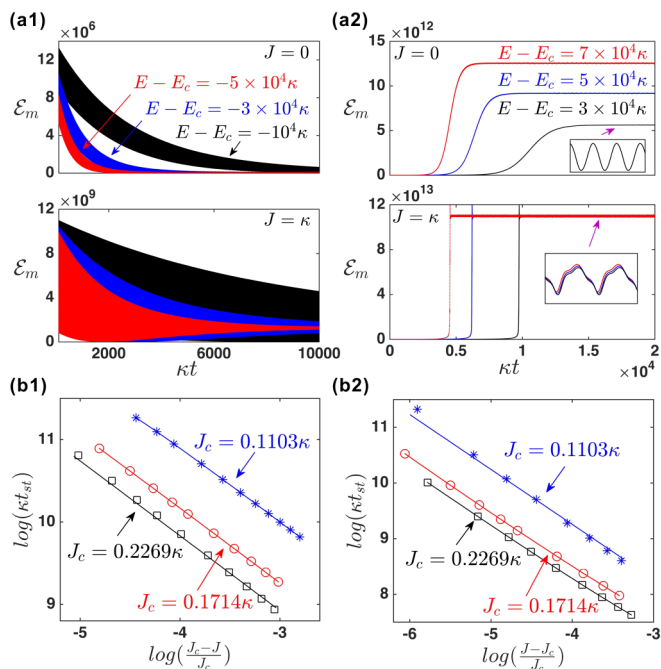


FIG. 3. (a1),(a2) The comparison of the critical slowing-down tendencies between those of a single-cavity setup with  $J = 0$  and a two-coupled-cavity setup with  $J = \kappa$ . The multimode pattern for  $\mathcal{E}_m(t)$  at  $J = \kappa$  is due to the large optomechanical force that renders the small displacement  $d$  in Eq. (4) time dependent. The evolutions are from a static initial condition and with the system constants in Fig. 1 except that  $g_0 = 0$ . (b1),(b2) The numerically obtained relations for determining the critical exponents.

In the situation of  $J = 0$ , there is a previously discovered scenario of sudden transition from a static steady state ( $A = 0$ ) to a stable oscillation ( $A \neq 0$ ) around the blue-detuned sidebands  $\Delta = -2\omega_m, -3\omega_m$ , etc. [65], which is connected with the possible existence of the multiple attractors of dynamics in the regime [43]. With the currently applied system parameters, for example, such a transition at  $\Delta = -2\omega_m$  requires a driving power equivalent to  $g_m E/\kappa^2 \approx 21$ . A special mechanism of the coupled cavities is to shift the sudden transition to near point X in Fig. 2(c1), where  $g_m E/\kappa^2 \approx 1$ , thus significantly altering the critical dynamics by very weak coupling between two microresonators. Another similar phenomenon is when a single-cavity optomechanical system is under an extremely strong driving field of resonance ( $\omega_l = \omega_c$ ) or two fields with the matched frequencies ( $\omega_{l,1} = \omega_c - \omega_m$  and  $\omega_{l,2} = \omega_c$ ) [66]. A tiny pumping power change in this case can cause the transition between two frozen mechanical orbits, but the transition, which becomes sensitive to the initial state of the system, belongs to a different category since there is no slowing-down behavior around the transition points.

There is an interesting observation on the dynamical evolutions without optical gain ( $g_0 = 0$ )—for the systems only differed by  $g_m$ , their dynamical evolution courses are similar under the condition  $g_m E = \text{constant}$  [67]. This rule of evolution applies to our concerned transition in that the transition point is determined by the product  $g_m E_c$ . If  $\mu R_1$  is replaced by another microresonator with a different  $g_m$ , the transition can still be realized by modifying the critical drive amplitude  $E_c$

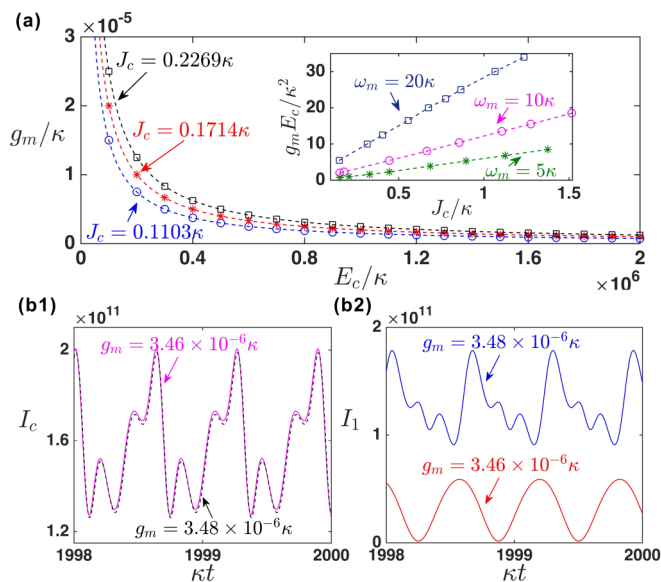


FIG. 4. (a) The transition locations in terms of  $g_m$  and  $E_c$ . The equations of the three curves (from the left to the right):  $g_m E_c = 1.5\kappa^2$ ,  $2.0\kappa^2$ , and  $2.5\kappa^2$ . The straight lines in the inset:  $g_m E_c/\kappa^2 = 12.1J_c/\kappa + 0.094$  (pink),  $g_m E_c/\kappa^2 = 6.415J_c/\kappa + 0.4156$  (green), and  $g_m E_c/\kappa^2 = 26.49J_c/\kappa + 1.773$  (black). At low  $J/\kappa$ , there are small deviations of such straight lines from the values of the product  $g_m E_c/\kappa^2$ . These relations are obtained with  $g_0 = 0$ . (b1),(b2) An example of discriminating two close values of the constant  $g_m$ . In a single cavity almost no difference exists in the field intensity  $I_c$ , but their field patterns will separate simply by coupling to another microresonator as in (b2). To show the clearer oscillation patterns, we here include the optical gain among the used system parameters from Fig. 1.

so that  $g_m E_c$  keeps invariant. The locations for the transition are thus summarized in Fig. 4(a) as the equation

$$g_m E_c/\kappa^2 = A(\omega_m)J_c/\kappa + B(\omega_m) \quad (8)$$

obtained from  $\mathcal{E}_m(0) = 0$ , where  $A(\omega_m)$  and  $B(\omega_m)$  are the coefficients. Within a certain range of the gain rate  $g_0$  and saturation rate  $I_S$ , the above relation holds approximately valid in the presence of the optical gain, so that the transition boundary in Fig. 2(c1) well fits into a straight line.

The optical gain in  $\mu R_2$  influences the system dynamics in some other aspects. Generally the saturated optical gain induces the field and mechanical oscillation before reaching the driving power for the concerned sudden transition. As a type of extra nonlinearity, the gain saturation interplays with the other factors and gives rise to more transition such as the one across point F in Fig. 2(c1), which is nontrivial. Moreover, the gain saturation speeds up the stability of the dynamical evolutions around the sudden transition point, modifying the slowing-down behaviors in the critical regime.

A useful application of the sudden transition is to measure the optomechanical constant  $g_m = x_{ZPF} \omega_c/R$ , with  $R$  being the cavity size. This parameter, which is proportional to a tiny zero-point fluctuation amplitude  $x_{ZPF} = \sqrt{\hbar/(m\omega_m)}$ , used to be measured by detecting a noise spectrum [74]. The linear relation between  $g_m E_c$  and  $J_c$  in Eq. (8) allows a more simplified measurement of  $g_m$  by finding the critical amplitude  $E_c$ ,

which is possible by a fine-tuning of the pump laser power. Figures 4(b1) and 4(b2) provide an example that  $g_m$  can be ascertained to a precision of  $10^{-8}\kappa$ . A tiny difference between two close values of  $g_m$  is magnified in the corresponding quantities of  $g_mE$ , which can locate on the different sides of a sudden transition, given a fixed coupling  $J$  to the second microresonator.

So far we have presented the main features of a dynamical transition in the setup illustrated in Fig. 1(a). To this coupler, a catastrophic drop of the cavity field intensities will suddenly manifest, if the distance between the two microresonators is reduced to a critical value. On the other hand, the field intensities will suddenly go up, together with the emergence of the high harmonic field components, when the pump laser power is increased to a certain value from zero. These observable phenomena correspond to a jump between two stable oscil-

lations of the mechanical mode, which undergoes a sudden change of its amplitude. Two slightly coupled microresonators make such transition take place under the lowered pump power. Interestingly the transition under the given system parameters can be affected by the initial condition. The setups previously made for a type of phonon laser can be developed into a platform to study the rich critical behaviors of such constantly oscillating system and their potential applications.

The authors thank Professor Zhigang Zheng at Huaqiao University (Xiamen) for the discussions on bifurcation of nonlinear systems. This work was supported by Fondo de Iniciación, Universidad Mayor de Chile (code PEP I-2019021), and National Natural Science Foundation of China (Grant No. 11574093).

- 
- [1] Y. A. Kuznetsov, *Elements of Applied Bifurcation Theory* (Springer, New York, 1998).
- [2] T. Ma and S. Wang, *Phase Transition Dynamics* (Springer, New York, 2014).
- [3] J. R. Tredicce, G. L. Lippi, P. Mandel, B. Charasse, A. Chevalier, and B. Picque, Critical slowing down at a bifurcation, *Am. J. Phys.* **72**, 799 (2004).
- [4] M. Scheffer, J. Bascompte, W. A. Brock, V. Brovkin, S. R. Carpenter, V. Dakos, H. Held, E. H. van Nes, M. Rietkerk, and G. Sugihara, Early-warning signals for critical transitions, *Nature (London)* **461**, 53 (2009).
- [5] E. Garmire, J. H. Marburger, S. D. Allen, and H. G. Winful, Transient response of hybrid bistable optical devices, *Appl. Phys. Lett.* **34**, 374 (1979).
- [6] J. Y. Bigot, A. Daunois, and P. Mandel, Slowing down far from the limit points in optical bistability, *Phys. Lett. A* **123**, 123 (1987).
- [7] B. A. Huberman and J. Rudnick, Scaling Behavior of Chaotic Flows, *Phys. Rev. Lett.* **45**, 154 (1980).
- [8] B.-L. Hao, Universal slowing-down exponent near period-doubling bifurcation points, *Phys. Lett. A* **86**, 267 (1981).
- [9] J. Guckenheimer and P. J. Holmes, *Nonlinear Oscillations, Dynamical Systems, and Bifurcations of Vector Fields* (Springer, New York, 1983).
- [10] L. Perko, *Differential Equations and Dynamical Systems* (Springer-Verlag, New York, 2001).
- [11] V. A. Gaiko, *Global Bifurcation Theory and Hilbert's Sixteenth Problem*, Mathematics and its Applications Vol. 559 (Kluwer Academic, Dordrecht, The Netherlands, 2003).
- [12] J. Moehlis, K. Josic, and E. Shea-Brown, Periodic orbit, *Scholarpedia* **1**, 1358 (2006).
- [13] M. Rasmussen, *Attractivity and Bifurcation for Nonautonomous Dynamical Systems* (Springer, New York, 2007).
- [14] F. Dercole and S. Rinaldi, Dynamical systems and their bifurcations, in *Advanced Methods of Biomedical Signal Processing*, edited by S. Cerutti and C. Marchesi (IEEE-Wiley Press, New York, 2011), pp. 291–325.
- [15] A. Capietto, P. Kloeden, J. Mawhin, S. Novo, and R. Ortega, *Stability and Bifurcation Theory for Non-Autonomous Differential Equations: Cetraro, Italy 2011* (Springer, New York, 2013).
- [16] S. H. Strogatz, *Nonlinear Dynamics and Chaos*, 2nd ed. (CRC Press/Taylor & Francis, Boca Raton/London, 2018).
- [17] H. K. Leung, Critical slowing down in synchronizing nonlinear oscillators, *Phys. Rev. E* **58**, 5704 (1998).
- [18] H. K. Leung, Bifurcation of synchronization as a nonequilibrium phase transition, *Physica A* **281**, 311 (2000).
- [19] P. Wofo and R. A. Kraenkel, Synchronization: Stability and duration time, *Phys. Rev. E* **65**, 036225 (2002).
- [20] J. A. Langa, J. C. Robinson, and A. Suárez, Stability, instability, and bifurcation phenomena in non-autonomous differential equations, *Nonlinearity* **15**, 887 (2002).
- [21] M. Marconi, J. Javaloyes, S. Balle, and M. Giudici, How Lasng Localized Structures Evolve out of Passive Mode Locking, *Phys. Rev. Lett.* **112**, 223901 (2014).
- [22] A. V. Kovalev and E. A. Viktorov, Class-A mode-locked lasers: Fundamental solutions, *Chaos* **27**, 114318 (2017).
- [23] P. Parra-Rivas, D. Gomila, L. Gelens, and E. Knobloch, Bifurcation structure of localized states in the Lugiato-Lefever equation with anomalous dispersion, *Phys. Rev. E* **97**, 042204 (2018).
- [24] S. Coen and M. Erkintalo, Universal scaling laws of Kerr frequency combs, *Opt. Lett.* **38**, 1790 (2013).
- [25] B. Haegeman, K. Engelborghs, D. Roose, D. Pieroux, and T. Erneux, Stability and rupture of bifurcation bridges in semiconductor lasers subject to optical feedback, *Phys. Rev. E* **66**, 046216 (2002).
- [26] J.-P. Francoise and C. C. Pough, Keeping track of limit cycles, *J. Diff. Equations* **65**, 139 (1986).
- [27] L. M. Perko, Global family of limit cycles of planar, *Trans. Amer. Math. Soc.* **322**, 627 (1990).
- [28] L. M. Perko, Homoclinic loop and multiple limit cycle bifurcation surfaces, *Trans. Amer. Math. Soc.* **344**, 101 (1994).
- [29] L. M. Perko, Multiple limit cycle bifurcation surfaces and global families of multiple limit cycles, *J. Diff. Equations* **122**, 89 (1995).
- [30] H. Xu, U. Kemiktarak, J. Fan, S. Ragole, J. Lawall, and J. M. Taylor, Observation of optomechanical buckling transitions, *Nat. Commun.* **8**, 14481 (2017).
- [31] A. Roy, S. Jahani, C. Langrock, M. Fejer, and A. Marandi, Spectral phase transitions in optical parametric oscillators, *Nat. Commun.* **12**, 835 (2021).

- [32] V. M. Bastidas, C. Emary, B. Regler, and T. Brandes, Non-Equilibrium Quantum Phase Transitions in the Dicke Model, *Phys. Rev. Lett.* **108**, 043003 (2012).
- [33] J. Klinder, H. Keßler, M. Wolke, L. Mathey, and A. Hemmerich, Dynamical phase transition in the open Dicke model, *Proc. Natl. Acad. Sci. USA* **112**, 3290 (2015).
- [34] Z. Zhang, C. H. Lee, R. Kumar, K. J. Arnold, S. J. Masson, A. S. Parkins, and M. D. Barrett, Nonequilibrium phase transition in a spin-1 Dicke model, *Optica* **4**, 424 (2017).
- [35] J. M. Fink, A. Dombi, A. Vukics, A. Wallraff, and P. Domokos, Observation of the Photon-Blockade Breakdown Phase Transition, *Phys. Rev. X* **7**, 011012 (2017).
- [36] N. Mann, M. R. Bakhtiari, A. Pelster, and M. Thorwart, Nonequilibrium Quantum Phase Transition in a Hybrid Atom-Optomechanical System, *Phys. Rev. Lett.* **120**, 063605 (2018).
- [37] C. Gao and Z. Liang, Steady-state phase diagram of quantum gases in a lattice coupled to a membrane, *Phys. Rev. A* **99**, 013629 (2019).
- [38] N. Mann, A. Pelster, and M. Thorwart, Tuning the order of the nonequilibrium quantum phase transition in a hybrid atom-optomechanical system, *New J. Phys.* **21**, 113037 (2019).
- [39] A. Dorsel, J. D. McCullen, P. Meystre, E. Vignes, and H. Walther, Optical Bistability and Mirror Confinement Induced by Radiation Pressure, *Phys. Rev. Lett.* **51**, 1550 (1983).
- [40] H. Rokhsari, T. Kippenberg, T. Carmon, and K. Vahala, Radiation-pressure-driven micro-mechanical oscillator, *Opt. Express* **13**, 5293 (2005).
- [41] T. J. Kippenberg, H. Rokhsari, T. Carmon, A. Scherer, and K. J. Vahala, Analysis of Radiation-Pressure Induced Mechanical Oscillation of an Optical Microcavity, *Phys. Rev. Lett.* **95**, 033901 (2005).
- [42] T. Carmon, H. Rokhsari, L. Yang, T. J. Kippenberg, and K. J. Vahala, Temporal Behavior of Radiation-Pressure-Induced Vibrations of an Optical Microcavity Phonon Mode, *Phys. Rev. Lett.* **94**, 223902 (2005).
- [43] F. Marquardt, J. G. E. Harris, and S. M. Girvin, Dynamical Multistability Induced by Radiation Pressure in High-Finesse Micromechanical Optical Cavities, *Phys. Rev. Lett.* **96**, 103901 (2006).
- [44] K. J. Vahala, Back-action limit of linewidth in an optomechanical oscillator, *Phys. Rev. A* **78**, 023832 (2008).
- [45] G. Heinrich, M. Ludwig, J. Qian, B. Kubala, and F. Marquardt, Collective Dynamics in Optomechanical Arrays, *Phys. Rev. Lett.* **107**, 043603 (2011).
- [46] A. G. Krause, J. T. Hill, M. Ludwig, A. H. Safavi-Naeini, J. Chan, F. Marquardt, and O. Painter, Nonlinear Radiation Pressure Dynamics in an Optomechanical Crystal, *Phys. Rev. Lett.* **115**, 233601 (2015).
- [47] J. Wen, X. Jiang, L. Jiang, and M. Xiao, Parity-time symmetry in optical microcavity systems, *J. Phys. B: At., Mol. Opt. Phys.* **51**, 222001 (2018).
- [48] R. El-Ganainy, K. G. Makris, M. Khajavikhan, Z. H. Musslimani, S. Rotter, and D. N. Christodoulides, Non-Hermitian physics and  $\mathcal{PT}$  symmetry, *Nat. Phys.* **14**, 11 (2018).
- [49] I. S. Grudinin, H. Lee, O. Painter, and K. J. Vahala, Phonon Laser Action in a Tunable Two-Level System, *Phys. Rev. Lett.* **104**, 083901 (2010).
- [50] H. Jing, S. K. Özdemir, X. Y. Lü, J. Zhang, L. Yang, and F. Nori,  $\mathcal{PT}$ -Symmetric Phonon Laser, *Phys. Rev. Lett.* **113**, 053604 (2014).
- [51] B. He, L. Yang, and M. Xiao, Dynamical phonon laser in coupled active-passive microresonators, *Phys. Rev. A* **94**, 031802(R) (2016).
- [52] H. Lü, S. K. Özdemir, L.-M. Kuang, F. Nori, and H. Jing, Exceptional Points in Random-Defect Phonon Lasers, *Phys. Rev. Appl.* **8**, 044020 (2017).
- [53] Y. L. Zhang, C. L. Zou, C. S. Yang, H. Jing, C. H. Dong, G. C. Guo, and X. B. Zou, Phase-controlled phonon laser, *New J. Phys.* **20**, 093005 (2018).
- [54] B. Wang, H. Xiong, X. Jia, and Y. Wu, Phonon laser in the coupled vector cavity optomechanics, *Sci. Rep.* **8**, 282 (2018).
- [55] Y. F. Xie, Z. Cao, B. He, and Q. Lin,  $\mathcal{PT}$ -symmetric phonon laser under gain saturation effect, *Opt. Express* **28**, 22580 (2020).
- [56] G. Z. Wang, M. M. Zhao, Y. C. Qin, Z. Q. Yin, X. S. Jiang, and M. Xiao, Demonstration of an ultra-low-threshold phonon laser with coupled microtoroid resonators in vacuum, *Photonics Res.* **5**, 73 (2017).
- [57] J. Zhang, B. Peng, Ş. K. Özdemir, K. Pichler, D. O. Krimer, G. P. Zhao, F. Nori, Y. X. Liu, S. Rotter, and L. Yang, A phonon laser operating at an exceptional point, *Nat. Photonics* **12**, 479 (2018).
- [58] B. He, L. Yang, X. Jiang, and M. Xiao, Transmission Nonreciprocity in a Mutually Coupled Circulating Structure, *Phys. Rev. Lett.* **120**, 203904 (2018).
- [59] Z. Cao, Y. F. Xie, B. He, and Q. Lin, Ultra-high optical nonreciprocity with a coupled triple-resonator structure, *New J. Phys.* **23**, 023010 (2021).
- [60] B. He, L. Yang, Q. Lin, and M. Xiao, Radiation Pressure Cooling as a Quantum Dynamical Process, *Phys. Rev. Lett.* **118**, 233604 (2017).
- [61] W. D. Heiss, The physics of exceptional points, *J. Phys. A: Math. Theor.* **45**, 444016 (2012).
- [62] V. V. Konotop, J. Yang, and D. A. Zezyulin, Nonlinear waves in  $\mathcal{PT}$ -symmetric systems, *Rev. Mod. Phys.* **88**, 035002 (2016).
- [63] M.-A. Miri and A. Alù, Exceptional points in optics and photonics, *Science* **363**, eaar7709 (2019).
- [64] Ş. K. Özdemir, S. Rotter, F. Nori, and L. Yang, Paritytime symmetry and exceptional points in photonics, *Nat. Mater.* **18**, 783 (2019).
- [65] M. Ludwig, B. Kubala, and F. Marquardt, The optomechanical instability in the quantum regime, *New J. Phys.* **10**, 095013 (2008).
- [66] B. He, Q. Lin, M. Orszag, and M. Xiao, Mechanical oscillations frozen on discrete levels by two optical driving fields, *Phys. Rev. A* **102**, 011503(R) (2020).
- [67] See Supplemental Material at <http://link.aps.org/supplemental/10.1103/PhysRevResearch.3.L032018>, which includes Refs. [68–73], for more detailed information.
- [68] L. Gammatoni, P. Hänggi, P. Jung, and F. Marchesoni, Stochastic resonance, *Rev. Mod. Phys.* **70**, 223 (1998).
- [69] W. Horsthemke and R. Lefever, *Noise-Induced Transitions* (Springer-Verlag, Berlin, Heidelberg, 2006).
- [70] Q. Lin, B. He, and M. Xiao, Entangling Two Macroscopic Mechanical Resonators at High Temperature, *Phys. Rev. Appl.* **13**, 034030 (2020).

- [71] B. He, L. Yang, Z. Zhang, and M. Xiao, Cyclic permutation-time symmetric structure with coupled gain-loss microcavities, *Phys. Rev. A* **91**, 033830 (2015).
- [72] B. He, S.-B. Yan, J. Wang, and M. Xiao, Quantum noise effects with Kerr-nonlinearity enhancement in coupled gain-loss waveguides, *Phys. Rev. A* **91**, 053832 (2015).
- [73] T. F. Roque, F. Marquardt, and O. M. Yevtushenko, Nonlinear dynamics of weakly dissipative optomechanical systems, *New J. Phys.* **22**, 013049 (2020).
- [74] M. L. Gorodetsky, A. Schliesser, G. Anetsberger, S. Deleglise, and T. J. Kippenberg, Determination of the vacuum optomechanical coupling rate using frequency noise calibration, *Opt. Express* **18**, 23236 (2010).